JOURNAL OF VIROLOGY, Feb. 2010, p. 1254–1264 Vol. 84, No. 3
0022-538X/10/$12.00 doi:10.1128/JVI.01533-09

Nuclear Import and Assembly of Influenza A Virus RNA Polymerase Studied in Live Cells by Fluorescence Cross-Correlation Spectroscopy▽†

Sébastien Huet,[1] Sergiy V. Avilov,[1,2,3] Lars Ferbitz,[2]‡ Nathalie Daigle,[1] Stephen Cusack,[2]* and Jan Ellenberg[1]*

Cell Biology and Biophysics Unit, European Molecular Biology Laboratory, Meyerhofstrasse 1, D-69117 Heidelberg, Germany[1]; Grenoble Outstation, European Molecular Biology Laboratory, 6 rue Jules Horowitz, 38042 Grenoble cedex 9, France[2]; and Palladin Institute of Biochemistry, 9 Leontovich str., Kiev 01030, Ukraine[3]

Received 23 July 2009/Accepted 4 November 2009

Intracellular transport and assembly of the subunits of the heterotrimeric RNA-dependent RNA polymerase constitute a key component of the replication cycle of influenza virus. Recent results suggest that efficient polymerase assembly is a limiting factor in the viability of reassortant viruses. The mechanism of nuclear import and assembly of the three polymerase subunits, PB1, PB2, and PA, is still controversial, yet it is clearly of great significance in understanding the emergence of new strains with pandemic potential. In this study, we systematically investigated the interactions between the polymerase subunits and their localization in living cells by fluorescence cross-correlation spectroscopy (FCCS) and quantitative confocal microscopy. We could show that PB1 and PA form a dimer in the cytoplasm, which is imported into the nucleus separately from PB2. Once in the nucleus, the PB1/PA dimer associates with PB2 to form the trimeric polymerase. Photon-counting histogram analysis revealed that trimeric polymerase complexes can form higher-order oligomers in the nucleus. We furthermore demonstrate that impairing the nuclear import of PB2 by mutating its nuclear localization signal leads to abnormal formation of the trimeric polymerase in the cytoplasm. Taken together, our results demonstrate which of the previously discussed influenza virus polymerase transport models operates in live cells. Our study sheds light on the interplay between the nuclear import of the subunits and the assembly of the influenza virus polymerase and provides a methodological framework to analyze the effects of different host range mutations in the future.

Influenza A viruses can infect a wide range of avian and mammalian species (49). Most avian strains of influenza virus infect wild waterfowl and domestic poultry but usually do not spread to humans. However, adaptation of pathogenic avian viruses to humans can occur either by mutation or reassortment, leading to potentially very serious pandemics, as was the case in 1918 when the "Spanish" flu caused 20 to 40 million deaths worldwide (33). Due to this ability to cross the species barrier, influenza A viruses are a permanent threat to human health. Since 2005 the spread of highly pathogenic H5N1 avian strains in Asia, Europe, and Africa has raised serious concern about the potential of this strain to cause an influenza pandemic (50). Since early 2009, an ongoing new, rapidly evolving pandemic threat has arisen from the emergence of a highly contagious, interhuman-transmissible "quadruple reassortant" swine H1N1 virus to which the world population is antigenically naïve (6).

Influenza A viruses are enveloped viruses of the orthomyxovirus family whose genomes comprise eight negative-strand RNA segments (2). In contrast to many RNA viruses, the influenza virus genome is transcribed and replicated by the trimeric viral RNA polymerase (PA, PB1, and PB2) in the nuclei of the infected cells. Therefore, the polymerase subunits, which are produced in the cytoplasm, have to be imported into the nucleus and assembled into a functional trimer (2, 18). Many studies have demonstrated that the viral polymerase plays a major role in host specificity, probably due to the necessity for the polymerase subunits to adapt to host cell-interacting partners such as nuclear import factors (13, 16, 25, 37, 46). Due to the lack of *in vivo* data concerning the interactions between the polymerase subunits in the nucleus and the cytoplasm of the host cells, the mechanisms of polymerase assembly and nuclear import, as well as their spatial and temporal relationships, are still not completely understood. Putative nuclear localization signals (NLSs) have been identified on PB1 (31), PB2 (29), and PA (32), suggesting that each subunit could be imported separately. However, based on *in vitro* assembly observations and cellular localization studies (8, 9, 12), it has been proposed that PB1 and PA are imported into the nucleus as a subcomplex by import factor RanBP5 (a member of the importin β superfamily). PB2 is thought to enter the nucleus separately, probably via the canonical importin α/importin β

* Corresponding author. Mailing address for Jan Ellenberg: Cell Biology and Biophysics Unit, European Molecular Biology Laboratory, Meyerhofstrasse 1, D-69117 Heidelberg, Germany. Phone: 49 6221 387-8328. Fax: 49 6221 387-8518. E-mail: jan.ellenberg@embl.de. Mailing address for Stephen Cusack: Grenoble Outstation, European Molecular Biology Laboratory, 6 rue Jules Horowitz, 38042 Grenoble cedex 9, France. Phone: 33 47620-7238. Fax: 33 47620-7786. E-mail: cusack@embl.fr.

† Supplemental material for this article may be found at http://jvi.asm.org/.

‡ Present address: Lonza Ltd., CH-3930, Visp, Switzerland.

▽ Published ahead of print on 11 November 2009.

pathway (46), and then associates with the PB1/PA heterodimer in the nucleus to form the functional trimeric polymerase. Nevertheless, alternative pathways have also been proposed. Naito et al. (30) suggested that the nuclear import of PB1 requires the formation of a PB2/PB1 heterodimer, stabilized by Hsp90, in the cytoplasm, while PA is transported in the nucleus separately. More recently, a pathway in which the PA/PB2 heterodimer would be formed in the cytoplasm and then imported into the nucleus has been proposed (17). It has also been recently shown that efficient assembly of the trimeric polymerase could be a major limiting factor in the viability of reassortant influenza viruses (26). Since gene reassortment is an evolutionary mechanism of influenza virus which can lead to new strains with pandemic potential, a precise understanding of the processes leading to the formation of an active viral polymerase in the nuclei of infected cells is of great importance.

Recent publications have demonstrated that fluorescence cross-correlation spectroscopy (FCCS) is a method of choice to study protein-protein interactions *in vivo* (23, 27, 42). FCCS is the dual-color extension of fluorescence correlation spectroscopy (FCS), a technique based on the analysis of the temporal fluorescence fluctuations arising from single fluorescently labeled molecules diffusing in and out of the femtoliter-scale detection volume commonly obtained with a confocal microscope. From the autocorrelation of the fluctuating signal, it is possible to extract the local concentrations and mobilities of the molecules of interest (10, 28, 39). In the case of FCCS, signals from two spectrally separated dyes labeling two different molecules are recorded. If the two molecules interact with each other, they diffuse synchronously through the detection volume, resulting in correlated fluctuations in the fluorescence signals acquired in the two channels. The cross-correlation between the two signals is then a direct and quantitative readout of the interactions between the molecular species studied (22, 38, 40). To our knowledge, this study is the first application of FCCS to viral protein interactions and thus provides a general methodological framework to analyze the effects of different host range mutations and the interactions of viral proteins and host factors in the future.

In this study, we applied FCCS to monitor the interactions between the subunits of influenza A virus RNA polymerase in live cells. Based both on the study of these interactions in the cytoplasm and nucleus and on the quantitative analysis of the intracellular localization of the subunits, we show that PB1 and PA form a heterodimer in the cytoplasm while PB2 remains a monomer in this compartment. Association of PB1/PA with PB2 to form the trimeric polymerase was detected only in the nucleus, arguing that the PB1/PA heterodimer is normally imported separately from PB2. Interestingly, when we impaired the nuclear import of PB2 by mutating its nuclear localization signal, this induced the aberrant presence of the trimeric polymerase in the cytoplasm and led to the retention of PB1 and PA outside the nucleus. Finally, by comparing the molecular brightnesses of the single polymerase subunits with that of the trimeric complex, we show that trimeric polymerase complexes can interact with each other in the nucleus to form higher-order oligomers.

MATERIALS AND METHODS

Fluorescent protein constructs. The Clontech Living Color plasmid backbone (Clontech, Mountain View, CA) was used to drive expression of fluorescently labeled PB1, PB2, and PA from influenza virus strain A/Victoria/3/75(H3N2) (7) in mammalian cells. For each construct, the entire coding sequence of the polymerase subunit was fused to the entire coding sequence of monomeric enhanced green fluorescent protein (mEGFP) (44), monomeric cyan fluorescent protein (mCFP) (a kind gift of J. Lippincott-Schwartz, National Institutes of Health, Bethesda, MD), or mCherry (41). It has been shown previously that GFP tags do not inhibit the transcriptional and replicative activities of the polymerase, except when fused at the N terminus of PB1 or PA (12). We therefore used PB1 and PA subunits tagged at the C terminus, and PB2 was tagged at its N terminus. pmEGFP-PB2 and pmEGFP-PB2-QNQ (a PB2 mutant with three point mutations [K738Q, K752N, and R755Q] at its C terminus [see Results]) have been described previously (46). In mCFP-PB2 and mCherry-PB2, an SGLRSRAQ linker connects the two fused proteins. In PB1-mEGFP, PB1-mCFP, and PB1-mCherry, the linker is AAAVPRARDPPVAT, and in PA-mEGFP, PA-mCFP, and PA-mCherry, it is TRDPPVAT.

Cell culture and transfection. HeLa Kyoto and A549 cells were routinely cultured in phenol-red free Dulbecco's modified Eagle's medium (4.5 g/liter glucose) supplemented with 10% fetal bovine serum, 2 mM glutamine, 100 μg/ml penicillin, 100 U/ml streptomycin, and 1 mM sodium pyruvate in 5% CO_2 at 37°C. At 48 h prior to experiments, cells were plated on LabTekII chambered cover glasses (Nunc, Roskilde, Denmark), and then they were transfected using Fugene 6 (Roche, Basel, Switzerland) or jetPRIME (Polyplus Transfection, Illkirch, France) 24 h later. For imaging and FCCS acquisitions, growth medium was replaced by a CO_2-independent medium without phenol red (Invitrogen, Carlsbad, CA) supplemented with 20% fetal bovine serum, 2 mM glutamine, 100 μg/ml penicillin, and 100 U/ml streptomycin. All the experiments were performed at 33°C.

Imaging and FCS/FCCS setup. Imaging and FCS/FCCS experiments were performed on a TCS SP2 acousto-optic beam splitter (AOBS) confocal microscope (Leica Microsystems, Wetzlar, Germany) using a water immersion Apochromat 63× objective lens (numerical aperture [NA], 1.2). The monomeric cyan fluorescent protein (mCFP) and the monomeric enhanced green fluorescent protein (mEGFP) were excited with the 458-nm and 488-nm lines of an argon laser, respectively. mCherry was excited using a 561-nm diode laser. For the FCS/FCCS acquisitions, the laser power at the sample level was set to approximately 1 μW for the different laser lines in order to minimize photobleaching. The size of the detection pinhole was set to 1 Airy unit. For imaging, fluorescence signals were detected using photomultiplier tubes. To separate the light emitted by the different fluorophores, the following spectral windows were chosen for the AOBS: 460 to 500 nm for mCFP, 500 to 550 nm for mEGFP, and 590 to 670 nm for mCherry. To minimize cross talk between mCFP and mEGFP, cells were first imaged in the cyan channel and then imaged simultaneously in the green and red channels. FCS/FCCS raw data were acquired using a specific detection module consisting of two avalanche photodiodes (APDs) (Perkin-Elmer Optoelectronics, Fremont, CA) coupled to a photon-counting card (ISS, Champaign, IL) allowing the registration of the raw intensity data at 24 MHz in the photon delay mode. Ahead of the APDs, fluorescence light was split using a dichroic mirror (LP560) and filtered spectrally by passing through band-pass emission filters (BP500-550 and HQ638DF75; Omega Optical, Brattleboro, VT). For each FCS/FCCS measurement, 2×10^5 to 5×10^5 photons were typically acquired.

FCS/FCCS data analysis. (i) Fitting of the FCS/FCCS curves. Auto/cross-correlation curves were calculated from raw intensity data using the FFS Dataprocessor 2.0 software (Scientific Software Technology Center, Minsk, Belarus). For time delays τ from 5 μs to 1 s, the auto/cross-correlation curves were fitted with a one-species model including the contribution of the fluorophore photophysics and assuming that the intracellular diffusion of the labeled subunits is anomalous (see the supplemental material for more details). From these fits of the autocorrelation curves, we could estimate the parameter N_{eff}, which refers to the mean number of fluorescent particles within the detection volume. For the cross-correlation curves, $N_{eff} = N_i N_j / N_{ij}$, where N_i, N_j, and N_{ij} are the mean numbers of particles within the detection volume detected in channel i, in channel j, and in both channels, respectively. As the size of the detection volume was equal to 0.7 to 1 fl (see the supplemental material), it was then possible to estimate the concentration of the labeled subunits in the probed cells.

The fits of the auto/cross-correlation curves also give access to the parameter τ_{diff}, which corresponds to the characteristic diffusion time of the fluorescent molecules within the detection volume. τ_{diff} depends both on the diffusion coefficient of the protein and on the size of the detection volume (40). Consequently, to analyze the diffusion properties of the influenza virus polymerase subunits, we

instead used the relative diffusion time given by $\tau_{diff,rel} = \tau_{diff}/\tau_{diff,mCherry}$, where $\tau_{diff,mCherry}$ is the diffusion time measured for uncoupled mCherry in the same compartment, which serves to calibrate the detection volume.

(ii) Determination of the proportion of the viral polymerase subunits engaged in a complex. FCCS was performed between the mEGFP- and the mCherry-labeled subunits. With our current setup, it was not possible to cross-correlate fluorescence signals from more than two channels. Consequently, when studying the formation of the trimeric polymerase complex, only the interactions between the mEGFP- and the mCherry-labeled subunits could be monitored by FCCS. The third subunit was labeled with mCFP to control its expression in the analyzed cell and to quantify its intracellular concentration (see the supplemental material for more details). In order to characterize the formation of dimeric or trimeric complexes between the polymerase subunits, we quantified the proportion of the least concentrated subunit engaged in a complex. For all these FCCS experiments, the least concentrated subunit was the mCherry-labeled one. The calculated proportions of subunit engaged in a complex were corrected for the nonperfect overlap between the detection volumes in the two channels and for the bleed-through from mEGFP into the red channel (see the supplemental material for more details).

Measurements of molecular brightness by photon-counting histogram analysis. The molecular brightness of the mEGFP-labeled polymerase subunits was estimated by photon-counting histogram (PCH) analysis. Raw intensity data were acquired using the same experimental settings as the ones used for FCS/FCCS acquisitions. Histograms of the numbers of photons per time bin of 100 μs were calculated from the raw intensity data using the FFS Dataprocessor 2.0 software. The photon histograms were fitted with a one-species model assuming a three-dimensional Gaussian detection volume (see the supplemental material for more details). From the analysis of the PCH curves, we estimated the mean number of fluorescent particles within the detection volume N_{eff}^{PCH} and the effective molecular brightness of these particles ε_{eff} (in counts per second per molecule). As the time binning used to calculate the photon histograms was in the same range as the characteristic time spent by the fluorescent molecules within the detection volume, the values obtained for N_{eff}^{PCH} and ε_{eff} had to be corrected for the diffusion of these molecules using the approach described by Perroud et al. (34). For the cells coexpressing the three fluorescently tagged polymerase subunits, we controlled by FCS that the mEGFP labeled subunit was the least concentrated one (see above).

Statistical analysis. For each quantitative analysis described in this study, the measurements were performed on 8 to 14 different cells per condition (for the FCCS experiments, this also includes measurements performed on positive and negative control cells [see the supplemental material for more details]). The values presented correspond to an average of these measurements and are given as mean ± standard deviations (SD). The significance of differences was calculated using Student's unpaired *t* test.

RESULTS

Influenza virus polymerase subunits influence each other's subcellular localization. Fluorescently labeled PB1, PA, and PB2 viral polymerase subunits were first expressed separately to study their intracellular localization. Strikingly, each of the three subunits showed a very different subcellular pattern. PB2 was localized nearly exclusively in the nucleus, while PA was present at similar concentrations in the cytoplasm and in the nucleus and PB1 was strongly accumulated in the cytoplasm (Fig. 1 and Table 1). While similar localization has been reported for PB2 and PA (12, 19, 46), the cytoplasmic localization of PB1 is in contrast with previous studies showing a nuclear or uniform distribution (30, 31, 43), which may be due to the use of cell lines from different organisms.

Next, we analyzed the localization of each polymerase subunit in the presence of its binding partners in all heterodimeric and trimeric combinations and quantitated the effect on the localization by measuring the nuclear/cytoplasmic concentration ratio (Fig. 1 and Table 1). In order to study how the localization of a given subunit is affected by the presence of another subunit(s) quantitatively, it was necessary to ensure that these subunits were in excess over the subunit whose localization was analyzed. We therefore measured the relative concentrations of all the subunits expressed in the cytoplasm of transfected cells by FCS, and the intracellular distribution of the subunit with the lowest cytoplasmic concentration was then monitored by quantitative confocal imaging. The localization pattern of PB1 and PA in the case of their coexpression was first characterized. Published reports suggest that these two subunits could be imported efficiently into the nucleus as a heterodimer (9, 12). Our experiments showed that when expressed together, PB1 and PA tended to relocalize into the nucleus, compared to the cells expressing only PA or PB1 (Fig. 1 and Table 1). The efficiency of the nuclear accumulation of these subunits was, however, quite low, as the nucleus/cytoplasm concentration ratios were lower than 2 for both PB1 and PA. Further, we studied how PB2 affects the intracellular distribution of either PB1 or PA. PB2 had no effect on the localization of PA or PB1.

Finally, the three polymerase subunits were coexpressed simultaneously. In the presence of their two binding partners, both PB1 and PA were localized nearly exclusively in the nucleus (Fig. 1 and Table 1). In order to control that the subunit localizations observed in HeLa cells were not specific to this cell line, we also analyzed these localizations in A549 cells (see Fig. S1 in the supplemental material). The results we obtained with A549 cells were similar to those with HeLa cells.

The observation that the nuclear accumulation of PB1 and PA is more efficient when both subunits are coexpressed in the presence of PB2 can be interpreted in two different ways: (i) the trimeric polymerase could be formed in the cytoplasm and then imported into the nucleus more efficiently than a PA/PB1 dimer, or (ii) PB1 and PA could be imported into the nucleus as a dimer and then interact with PB2 to form the trimeric polymerase; this association with PB2 would lead to the retention of PA and PB1 in the nucleus. In order to determine which of these models properly describes the mechanism occurring *in vivo*, we used fluorescence cross-correlation spectroscopy to visualize the interactions between the influenza virus polymerase subunits directly.

Interactions between the influenza virus polymerase subunits measured by fluorescence cross-correlation spectroscopy. In order to validate the FCCS method for measuring protein-protein interactions in live cells, we first performed FCCS measurement in cells expressing a construct for which mEGFP was physically linked to mCherry through a neutral spacer, the maltose-binding protein (positive control), and in cells coexpressing mEGFP and mCherry (negative control). For the positive controls we obtained strong cross-correlation signals both in the nucleus and in the cytoplasm (Fig. 2A, left). The amplitude of the cross-correlation curves was, however, about half of that of the auto-correlation curves in the green and red channels, revealing the imperfect overlap between the two excitation volumes. The subsequent measurements of the interactions between the influenza virus polymerase subunits were corrected for this artifact (see the supplemental material). For the negative controls, the amplitude of the cross-correlation curves was close to zero (Fig. 2A, middle). The very weak cross-correlation signal observed in these cells is due to the bleed-through from the mEGFP fluorescence into the red channel. This artifact was corrected when quantifying the in-

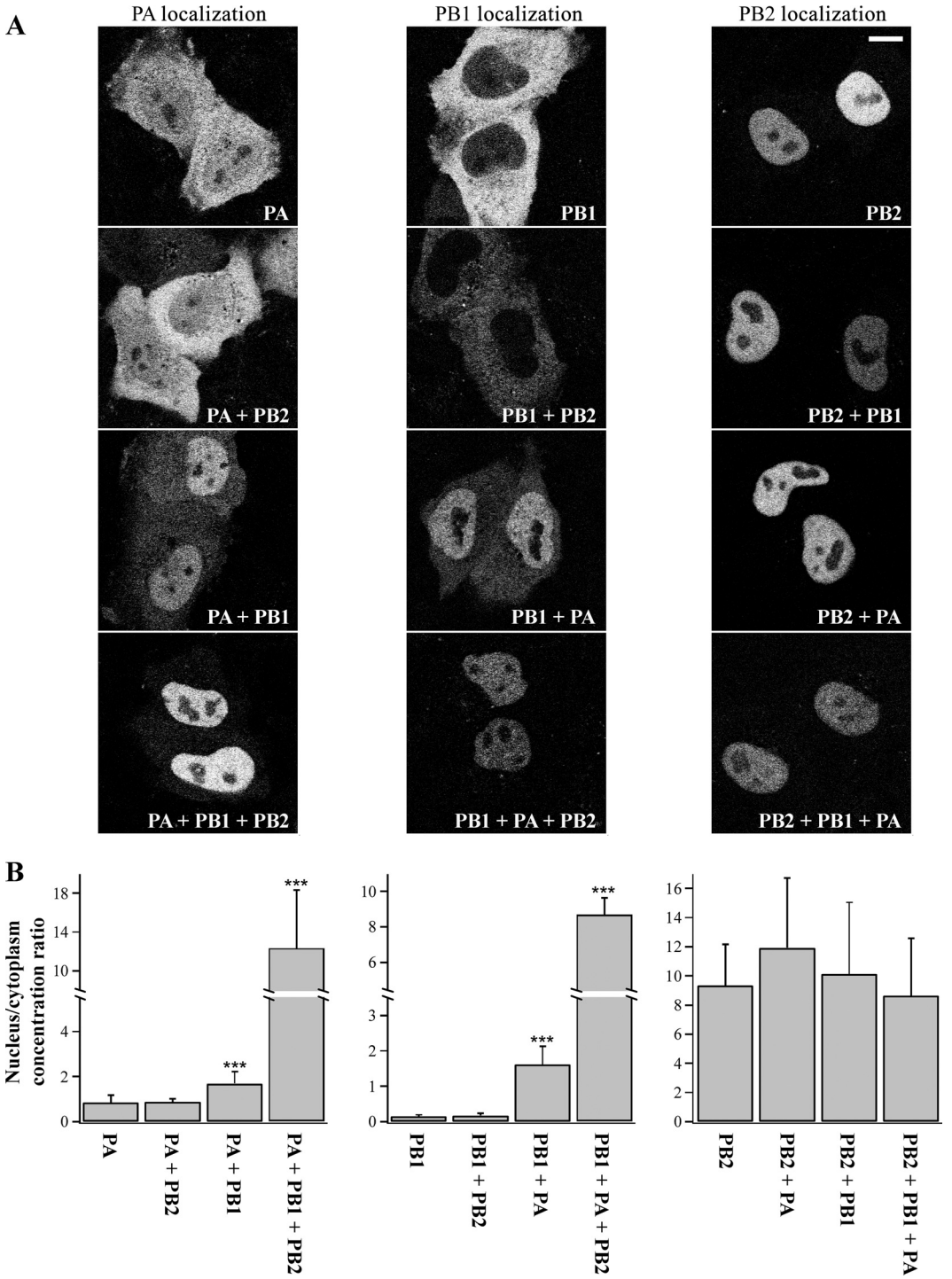

FIG. 1. Subcellular localization of the influenza virus polymerase subunits. (A) Subcellular localizations of PA-mEGFP (left column), PB1-mEGFP (center column), and mEGFP-PB2 (right column) when expressed alone or in association with other subunits in HeLa Kyoto cells. The legend at the bottom right of each image refers to the different subunits expressed by the cells. When two subunits were present, the subunit not shown was labeled with mCherry. In cells coexpressing the three subunits, the subunits not shown were labeled with mCherry and mCFP. This allowed to control by FCS that the shown subunit was the least concentrated in the cytoplasm. The autofluorescence was removed from the images by spectral linear unmixing (52). Scale bar, 10 μm. (B) Concentration ratio between the nucleus and the cytoplasm quantified from the confocal images for PA (left), PB1 (center), and PB2 (right) in cells expressing different combinations of subunits. For cells expressing multiple subunits, the subunit whose nucleus/cytoplasm concentration ratio was estimated was the least concentrated in the cytoplasm as assessed by FCS. ***, $P < 0.001$.

TABLE 1. Quantification of subcellular localizations of influenza virus polymerase subunits

Expressed subunit(s)	Ratio (mean ± SD) between nuclear and cytoplasmic concn for probed subunit[a]:			
	PA	PB1	PB2	PB2-QNQ
PA	0.8 ± 0.3			
PB1		0.2 ± 0.1		
PB2			9 ± 3	
PA + PB1	1.7 ± 0.5	1.6 ± 0.5		
PA + PB2	0.9 ± 0.2		12 ± 5	
PB1 + PB2		0.2 ± 0.1	10 ± 5	
PA + PB1 + PB2	12 ± 6	9 ± 1	9 ± 4	
PB2-QNQ				2.6 ± 0.6
PA + PB2-QNQ	0.8 ± 0.2			ND
PB1 + PB2-QNQ		0.3 ± 0.4		ND
PA + PB1 + PB2-QNQ	1.2 ± 0.6	0.8 ± 0.6		1.9 ± 0.6

[a] Ratio between the nuclear and cytoplasmic concentrations quantified from the confocal images. For cells expressing multiple subunits, the relative concentrations of the different subunits were first measured by FCS, and then the localization of the least concentrated subunit in the cytoplasm was quantified. ND, not determined.

teractions between the influenza virus polymerase subunits (see the supplemental material).

We then studied by FCCS the interactions between the different polymerase subunits in the cytoplasm and the nuclei of live HeLa cells (see Fig. 2A, right, for an example of the experimental auto/cross-correlation curves and Fig. 2B and C for the quantitative results). For these experiments, the intracellular concentrations of the different subunits were in the range of 10 to 100 nM, as shown by the analysis of the autocorrelation curves (see Materials and Methods). First, FCCS experiments were performed with cells coexpressing PB1 and PA to study the interactions between these two subunits. We found that almost all the PA subunit (which was the least concentrated subunit in these experiments) was in complex with PB1, with no significant difference ($P = 0.31$) between cytoplasm (87% ± 16% of PA in complex) and nucleus (93% ± 10% of PA in complex). In contrast, no significant interaction was observed between PA and PB2 in either the nucleus or the cytoplasm. In cells coexpressing PB2 and PB1, we observed that 28% ± 13% and 10% ± 14% ($P = 0.002$) of the least concentrated subunit (PB2 subunit for the measurements in the cytoplasm and PB1 subunit for the measurements in the nucleus) were engaged in a complex with its counterpart in the cytoplasm and in the nucleus, respectively. Finally, FCCS experiments were performed with cells coexpressing the three polymerase subunits (Fig. 2B and C). Since when expressed together, PB1 and PA form a heterodimer both in the cytoplasm and in the nucleus, we studied by two-color FCCS the interactions between PB2 and PB1 or between PB2 and PA in the presence of their third counterpart, assuming that PB1 and PA were in complex wherever they were coexpressed. The two subunits whose interactions were monitored were tagged with mEGFP and mCherry, while the third one was tagged with mCFP to control its expression in the analyzed cell and estimate its concentration. In the cytoplasm, we found no significant interactions between PB2 and PA in the presence of PB1. In contrast, 94% ± 21% of the PA subunit was in complex with PB2 in the nuclei of cells coexpressing the three subunits. Similar results were obtained when monitoring the interactions between PB2 and PB1 in the presence of PA (data not shown). These results show that while PB2 does not associate with the PA/PB1 dimer in the cytoplasm, the three subunits interacts with each other in the nucleus to form the trimeric polymerase. Together with the quantitative analysis of the intracellular localizations of the subunits, these observations suggest that PB2 and the PB1/PA dimer are imported separately into the nucleus, where they associate to form the trimeric polymerase.

Impairing nuclear import of PB2 leads to the formation of the trimeric polymerase in the cytoplasm. In order to investigate the role of nuclear import of the influenza virus polymerase subunits for the assembly of the trimeric complex further, we studied the impact of impairing the nuclear import of PB2 on the interactions between the subunits and their intracellular localizations. As reported previously (46), we observed that the triple mutation of the C-terminal NLS domain of PB2 (K738Q, K752N, and R755Q, hereafter referred as PB2-QNQ) strongly reduced its nuclear accumulation (Fig. 3A and Table 1). We then studied how PB2-QNQ affected the intracellular localization of PA and PB1. In contrast to the case for the wild-type PB2, coexpression with PB2-QNQ did not lead to the accumulation of PA and PB1 in the nucleus (Fig. 3A and Table 1). To assess formation of the trimeric complex, we then measured the interactions between PB2-QNQ and PA in cells coexpressing the three subunits by FCCS and found that 84% ± 17% and 90% ± 33% of the PA subunit (which was the least concentrated subunit in these experiments) were engaged in a complex with PB2-QNQ in the cytoplasm and in the nucleus, respectively (Fig. 3B and C). Control experiments performed in the absence of PB1 showed no significant interaction between PA and PB2-QNQ in the cytoplasm (data not shown). These results indicate that, in contrast to the wild-type PB2, PB2-QNQ, whose nuclear import is compromised, is able to interact with the PB1/PA dimer not only in the nucleus but also in the cytoplasm.

The trimeric influenza virus polymerase forms higher-order oligomers in the nucleus. Using our FCS/FCCS measurements, we could also characterize the diffusion of the wild-type polymerase subunits by estimating their relative diffusion times, $\tau_{diff,rel}$ (absolute diffusion time of the subunit divided by that of the uncoupled mCherry [see Materials and Methods]), in the nuclei and the cytoplasm of HeLa cells (Fig. 4). When expressed separately, PB1 and PA showed relative diffusion times of ~15 and ~3, respectively, both in the cytoplasm and in the nucleus. For PB2, $\tau_{diff,rel}$ was equal to 5 ± 2 in the cytoplasm and 11 ± 2 in the nucleus. Since in cells coexpressing PB1 and PA the proportion of the least concentrated, mCherry-labeled, subunit engaged in the PB1/PA dimer was close to 100%, the diffusion time of the PB1/PA dimer can be considered to be equal to that of the mCherry-labeled subunit. We thus find that the PB1/PA dimer diffused approximately 15 times slower than the uncoupled mCherry fluorophore both in the nucleus and in the cytoplasm. Using the same approach, we estimate that in the nucleus, the diffusion time of the trimeric polymerase was 1 order of magnitude slower than that of the mCherry control. Based on their molecular weights and assuming that they show a globular shape, the Stokes-Einstein hydrodynamic theory (51) predicts that the single subunits, the PB1/PA dimer, and the trimeric complex should diffuse ~1.6, ~2, and ~2.3 times

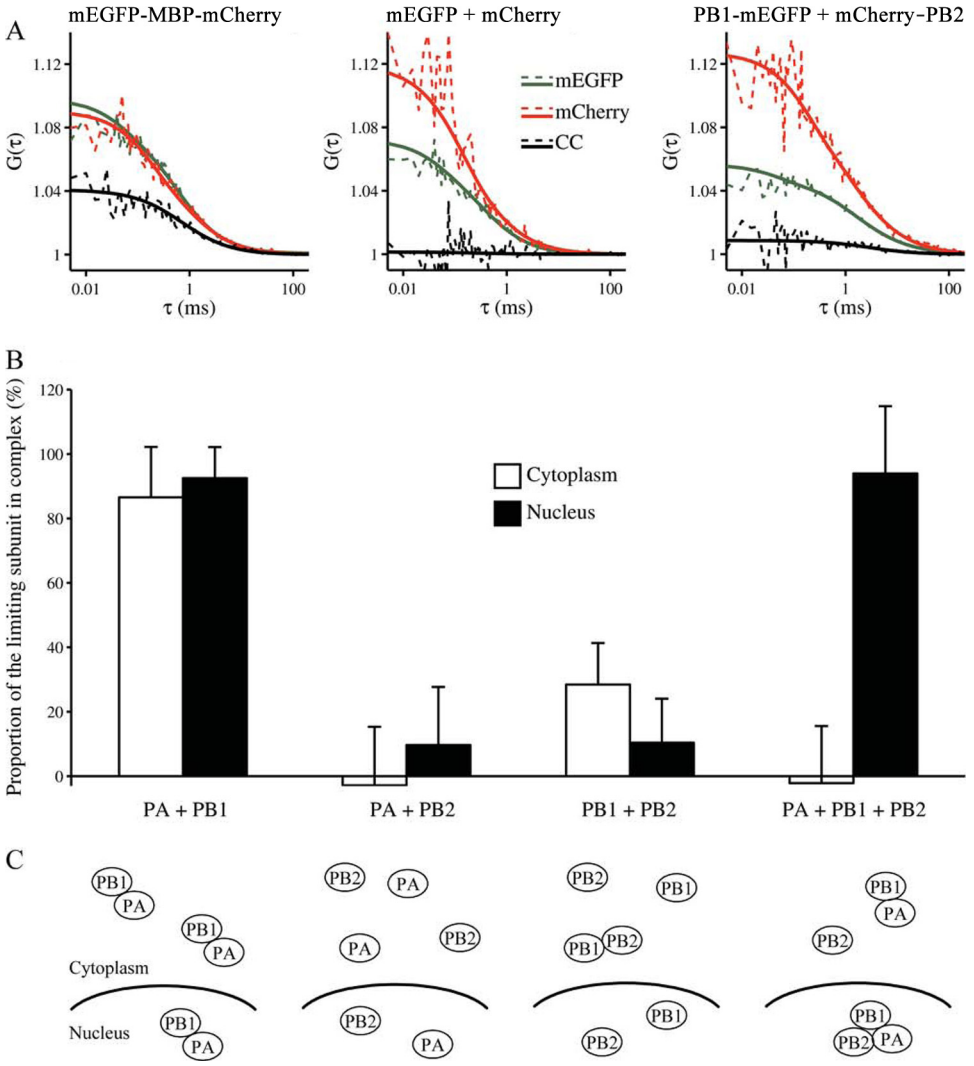

FIG. 2. Interactions between the influenza virus polymerase subunits studied by FCCS. (A) Examples of auto/cross-correlation curves measured in the cytoplasm of HeLa Kyoto cells expressing mEGFP-MBP-mCherry (left), mEGFP and mCherry (center), or PB1-mEGFP and mCherry-PB2 (right). The autocorrelation curves in the mEGFP and mCherry channels are shown in green and red, respectively. The cross-correlation (CC) curves are shown in black. The experimental curves (dotted lines) are fitted (solid lines) using a model assuming anomalous diffusion and, for the autocorrelation curves, accounting for the photophysics of the fluorophores. (B) Proportion of the limiting subunit engaged in a complex measured by FCCS in the cytoplasm and nuclei of HeLa Kyoto cells coexpressing pairs of subunits or the three subunits. In the double-expressing cells, the interactions between the mEGFP- and the mCherry-labeled subunits were directly analyzed by FCCS. When the three subunits were coexpressed, only the interaction between PA-mCherry and mEGFP-PB2 was monitored by FCCS. The presence of PB1-mCFP was assessed by imaging the cell in the CFP channel. For the FCCS measurements of the interactions between PA and PB1 or between the three subunits, the least concentrated subunit was PA. For the analysis of the interactions between PA and PB2, the least concentrated subunit was PB2 for the measurements in the cytoplasm and PA for the measurements in the nucleus. For the analysis of the interactions between PB1 and PB2, the least concentrated subunit was PB2 for the measurements in the cytoplasm and PB1 for the measurements in the nucleus. (C) Schematic description of the interactions observed by FCCS.

slower than the mCherry tag, respectively. The large discrepancies between these predictions and the measured diffusion characteristics of PB1, PB2, the PA/PB1 dimer, and the trimeric polymerase suggest that these different entities either exist in larger complexes with host factors or form higher-order homo-oligomers, or both.

We therefore investigated the potential formation of homo-oligomers in the nucleus using the photon-counting histogram (PCH) method. While FCS is based on a temporal analysis of the intensity fluctuations arising from single fluorescently labeled molecules diffusing in and out the detection volume, PCH instead characterizes the amplitude of these fluctuations. PCH analysis gives access to the brightness and the concentration of the fluorescent diffusing particles (4). As a homo-oligomer formed by *n* labeled proteins is expected to be *n*-fold brighter than a single labeled protein, PCH is a powerful tool to monitor homo-oligomerization. In order to validate the method in the context of *in vivo* measurements, we first compared the brightness of the uncoupled mEGFP tag with that of an mEGFP-mEGFP tandem. As expected, the tandem con-

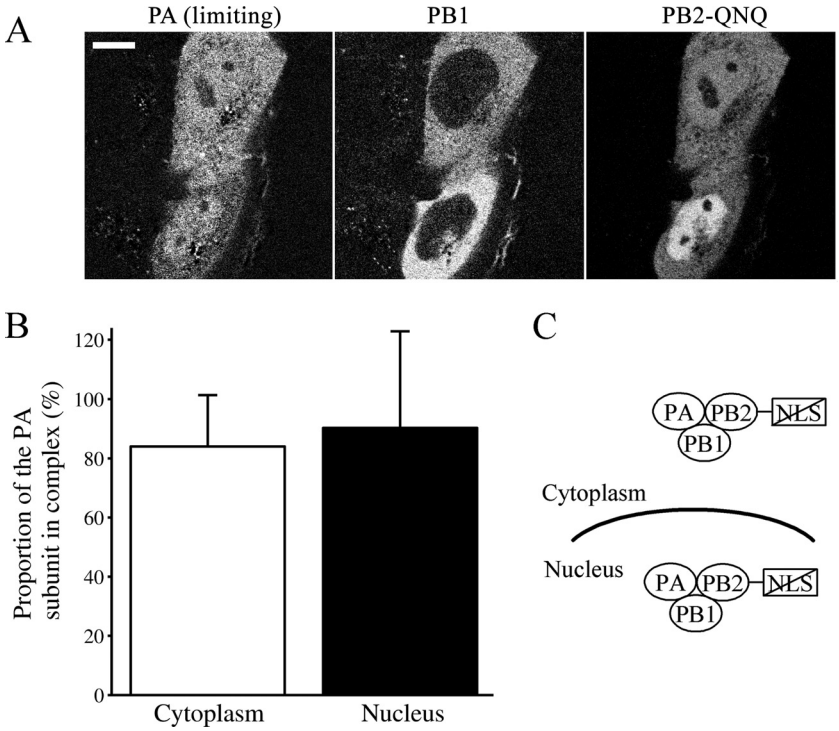

FIG. 3. Impact of mutating the nuclear localization signal of PB2 on subcellular localization and assembly of the trimeric polymerase. (A) Subcellular localizations of PA-mCherry (left), PB1-mCherry (center), and mEGFP-PB2-QNQ (right) in HeLa Kyoto cells coexpressing the three subunits. The PA subunit was the least concentrated one in the cytoplasm. The autofluorescence was removed from the images by spectral linear unmixing. Scale bar, 10 μm. (B) Proportion of PA-mCherry subunits interacting with mEGFP-PB2-QNQ measured by FCCS in the cytoplasm and the nuclei of HeLa Kyoto cells coexpressing PA-mCherry (least concentrated subunit), PB1-mCFP, and mEGFP-PB2-QNQ. (C) Schematic description of the interactions observed by FCCS.

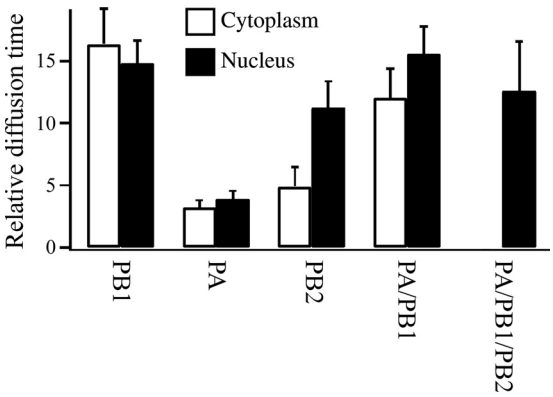

FIG. 4. Nuclear and cytoplasmic diffusions of the single influenza virus polymerase subunits, PB1/PA dimers, and trimeric complexes. The characteristic diffusion times of the mCherry-labeled subunits within the detection volume were estimated by fitting the autocorrelation curves obtained in the mCherry channel. Shown is the ratio between these diffusion times and those measured for uncoupled mCherry in the same compartment. These relative diffusion times were measured in the cytoplasm and in the nuclei of HeLa Kyoto cells. To characterize the diffusion of the PB1/PA dimer, the diffusion time of PA-mCherry was estimated in cells coexpressing PA-mCherry (least concentrated subunit) and PB1-mEGFP. As FCCS experiments showed that most of the PA-mCherry belongs to the PB1/PA dimer, the diffusion time of the PB1/PA dimer was considered to be equal to that of PA-mCherry. The same approach was used to estimate the nuclear diffusion time of the trimeric complex.

struct had nearly twice the brightness of mEGFP (Fig. 5). Next, we quantified by PCH the brightnesses of PA-mEGFP, PB1-mEGFP, and mEGFP-PB2 in the nuclei of cells expressing these different subunits separately (Fig. 5). In cells expressing PA-mEGFP or mEGFP-PB2, the brightness of the mEGFP-labeled particles was slightly but significantly increased ($P < 0.05$) compared to that of uncoupled mEGFP. This increased brightness may indicate a small tendency of PA-mEGFP and mEGFP-PB2 to form homo-oligomers, but we cannot exclude that it is rather due to the coupling of mEGFP to the polymerase subunits, which may slightly affect the brightness properties of mEGFP. While the brightness of PA-mEGFP was not affected by the coexpression of PB1-mCherry, expressing PA-mEGFP together with both PB1-mCFP and mCherry-PB2 induced an increase of ~35% in the brightness of the mEGFP-labeled particles compared to cells expressing only PA-mEGFP ($P < 0.001$). We controlled that this increase was not due to bleed-through from the mCherry and mCFP tags into the green channel (see the supplemental material). This observation suggests that the trimeric polymerase forms homo-oligomers in the nuclei of HeLa Kyoto cells. The formation of such higher-order oligomers should lead to an increase in molecular brightness proportional to the number of polymerases composing these oligomers. The fact that we observed only an ~35% increase of the molecular brightness in cells expressing the three subunits compared to those expressing only PA-mEGFP thus indicates that only a fraction of the

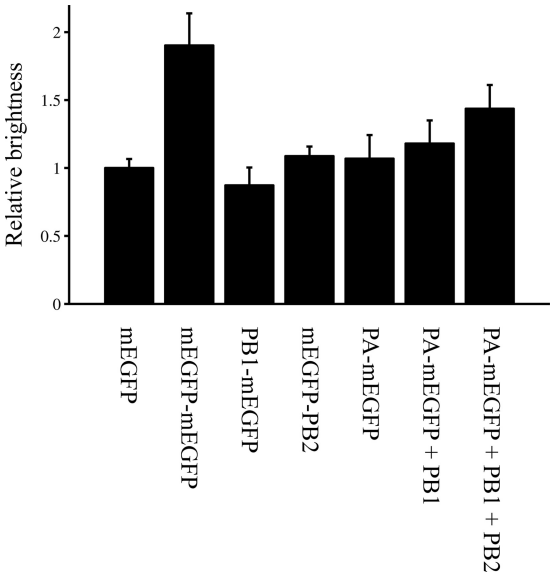

FIG. 5. Homo-oligomerization of the trimeric polymerase studied by PCH. The brightnesses of mEGFP-labeled particles were measured by PCH in the nuclei of cells expressing uncoupled mEGFP, the mEGFP-mEGFP tandem, or different combinations of the polymerase subunits. In cells coexpressing PA and PB1, PA was tagged with mEGFP and PB1 with mCherry. In cells coexpressing the three subunits, PA, PB1, and PB2 were labeled with mEGFP, mCFP, and mCherry, respectively. Shown is the ratio between these brightnesses and that of the uncoupled mEGFP.

polymerases are engaged in higher-order complexes. We confirmed the ability of the trimeric polymerase to form homo-oligomers by monitoring the interactions between mEGFP-PB2 and mCherry-PB2 by FCCS. While no cross-correlation signal could be detected in the nuclei of cells expressing only the two versions of the PB2 subunit, indicating no detectable interaction, we observed a positive cross-correlation signal in the presence of the other two subunits, PB1-mCFP and PA-mCFP. For these experiments, however, it was difficult to quantify the interactions between the trimeric polymerases as estimated previously based on the amplitudes of the auto/cross-correlation curves. Indeed, the different PB2 subunits contained in an oligomer formed by several polymerases can all be labeled with the same color. Such an oligomer will not contribute to the cross-correlation signal, leading to an underestimation of the interaction. Consequently, we only estimated the ratio between the cross-correlation curves and the auto-correlation curves in the green channel (see Fig. S2 in the supplemental material).

DISCUSSION

FCCS is a powerful tool to study the interactions between the influenza virus polymerase subunits *in vivo*. So far, the cellular processes leading to the assembly of a functional influenza virus RNA polymerase inside the nucleus have been studied mostly by *in vitro* biochemical techniques and imaging of fixed cells. As these techniques could not monitor the interactions between the polymerase subunits in living cells, the role of nuclear import in the assembly of the influenza virus polymerase has so far remained controversial. With this report, we show that FCCS coupled with quantitative confocal imaging and PCH analysis can be a very valuable tool to measure the interactions between the three influenza virus polymerase subunits *in vivo*. Using this approach, we found direct evidence for an assembly model according to which PB1 and PA heterodimerize in the cytoplasm and are independently imported as a binary complex into the nucleus, where formation of the functional PA/PB1/PB2 heterotrimer occurs through association of PB1/PA with independently imported PB2 (Fig. 6). This provides a direct *in vivo* confirmation of the model originally proposed by Deng et al. (9).

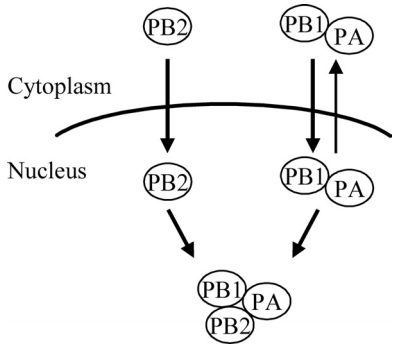

FIG. 6. Model of the nuclear import and assembly of the influenza virus RNA polymerase. The heterodimer formed by PA and PB1 is imported in the nucleus separately from PB2. Once in the nucleus, PB2 binds to PB1/PA to form the trimeric polymerase.

Nuclear import and assembly of the polymerase trimeric complex. In agreement with previous reports (12, 30), we observed that the efficient accumulation of PB2 inside the nucleus does not require the presence of other viral proteins. We confirmed that the nuclear import of PB2 depends to a significant extent on its C-terminal NLS (37, 46). We also found that the individually expressed PA and PB1 can enter the nucleus, in agreement with previous studies (1, 12, 19), but do not accumulate efficiently in this compartment, in contrast to PB2. When coexpressed, PA and PB1 display a moderate nuclear accumulation, in qualitative agreement with previous studies (12, 32). Deng and coauthors postulated that PA and PB1 are imported as a complex based on *in vitro* assembly experiments (9). Our present FCCS experiments show that this is indeed the case *in vivo*. We demonstrate that, both in the cytoplasm and in the nucleus, almost 100% of the least concentrated subunit (either PB1 or PA) is engaged in a PB1/PA complex. In contrast to the coimport of PB1 and PA, we did not observe any increase in the nuclear accumulation of PA in the presence of PB2. In addition, FCCS experiments detected no PB2/PA complexes, in agreement with several reports showing the lack of direct contacts between PA and PB2 (15, 35, 47, 48). In contrast to these results, an interaction between PB2 and PA has recently been detected using bimolecular fluorescence complementation (BiFC) (17). However, the biological relevance of this observation remains questionable, as BiFC irreversibly "locks in" even very transient interactions (5). Further, we observed that PB2 did not increase the nuclear accumulation of PB1, in agreement with some previous results (12) but in contrast to others which reported an increase of the nuclear accumulation of PB1 in the presence of PB2 at equal or higher

expression levels of the plasmid encoding PB2 (30). This discrepancy may be explained by the much higher subunit concentrations in transfected cells used for classical fluorescence imaging than in those suitable for FCS/FCCS experiments. Alternatively, it is also possible that the labeling of the polymerase subunits with fluorescent proteins partially preclude the interaction of these subunits with host nuclear import factors, thus impairing the potential coimport of PB2 and PB1 in the nucleus. Our FCCS measurements showed that only a minor portion of PB1 (28% and 10% in the cytoplasm and the nucleus, respectively) appeared within a complex with PB2, confirming the relatively weak interaction between PB1 and PB2 already reported (9). It is thus likely that the strong interface that can be formed between the N-terminal extremity of PB2 and the C-terminal extremity of PB1 (45) is present only in the fully assembled trimeric polymerase.

It was previously observed that coexpressed PA and PB2 improved nuclear accumulation of PB1 (12). However, only the combined effect of coexpressed PB2 and PA was tested and no comparison between the localization of PB1 in the presence of PA only and in the presence of both PA and PB2 was possible. In contrast, we compared triple coexpression (PB1, PB2, and PA) with all combinations of double coexpression and found that nuclear accumulation of coexpressed PB1 and PA is significantly increased in the presence of PB2. Furthermore, we could show for the first time that not only the presence of PB2 but also its ability to be efficiently imported into the nucleus is important, because the NLS-impaired mutant PB2-QNQ did not increase the nuclear accumulation of PB1 and PA, although PB2-QNQ retained the ability to form a trimeric complex. One possible explanation for the effect of PB2 on the localization of PB1 and PA is the formation of the heterotrimeric polymerase in the cytoplasm and its subsequent nuclear import driven by the NLS of PB2. Although in the FCCS experiments we did not detect any trimeric complexes in the cytoplasm, we cannot exclude the possibility that cytoplasmic heterotrimers are very efficiently imported into the nucleus after assembly and therefore their steady-state concentration in the cytoplasm is kept low. However, nuclear import of fully assembled stable trimers as the main route of transport for influenza virus polymerase appears unlikely, because RanBP5 (8) and Hsp90 (30) efficiently compete with trimer formation and because of the selective effect of Hsp90 inhibition on nuclear import of PB1/PA but not PB2 (3). Furthermore, although a minor fraction of PB1/PB2 dimers forms in the cytoplasm when these subunits are expressed alone, this did not lead to increased nuclear accumulation of PB1, suggesting that PB1 is not "carried" into the nucleus by the PB2 NLS. Therefore, we favor a model where the PB1/PA dimer and PB2 have independent transport routes into the nucleus (Fig. 6). Consequently, formation of the trimeric polymerase would normally occur in the nucleus and retain the subunits in the nucleus, leading to an efficient nuclear accumulation of PB1 and PA. The necessity to form heterotrimers in the nucleus to retain PB1 and PA may contribute to the poor replication activity of various "reassortant" polymerases composed of functionally "normal" subunits originating from different strains that are not optimally compatible in assembly (26).

Importin α-mediated nuclear import of PB2 may prevent aberrant formation of the trimeric polymerase in the cytoplasm. Competition between host factor binding and association of polymerase subunits has been previously reported. For instance, PB2 binds PB1/PA after the nuclear import factor RanBP5 dissociates from PB1/PA dimer (9), and Hsp90 was found bound to the PB1/PB2 dimer and PB2 alone, but this binding was strongly reduced in the presence of PA, allowing the formation of the PB2/PB1/PA heterotrimer (30). Here, we show that mutating the PB2 NLS, which mediates binding to importin alpha (46), leads to the aberrant presence of the trimeric polymerase in the cytoplasm. This observation can be interpreted in two different ways. (i) The binding of the wild-type PB2 to importin alpha in the cytoplasm and its subsequent rapid nuclear import could be a mechanism to prevent the formation of the trimer in the wrong compartment. In the nucleus, PB2 dissociation from the import factors by RanGTP would then enable the formation of the correctly localized, functional heterotrimer. For the PB2-QNQ mutant, its compromised interaction with the importin alpha in the cytoplasm would induce the aberrant formation of the trimeric polymerase in this compartment. (ii) Alternatively, the complex PB2-QNQ/PA/PB1 could still form specifically in the nucleus, similarly to the wild-type trimer, but then would leak or be transported back into the cytoplasm. The efficient nuclear accumulation of PB2 would thus be required for the correct localization of the trimeric polymerase inside the nucleus. Together, these results emphasize the importance of the C-terminal NLS of PB2, mutation of which impairs the nuclear accumulation of all polymerase subunits. However, it should be noted that the severe reduction of viral RNA replication for the PB2-QNQ mutant may not be solely explained by impaired nuclear accumulation, because restoration of nuclear localization of PB2-QNQ by an alternative nuclear import mechanism did not restore the replication efficiency (37).

The trimeric influenza virus polymerase forms higher-order oligomers in the nucleus. Our photon-counting histogram experiments showed that a fraction of the trimeric polymerase complexes interact with each other in the nucleus to form oligomers. Thus, we provide direct *in vivo* confirmation for the homo-oligomerization of influenza virus polymerase, which was recently suggested on the basis of *in vitro* studies of TAP-purified polymerase subunits (20). It has been proposed that the interactions between the polymerase present in the ribonucleoprotein particles and the incoming polymerase molecule may facilitate binding of the latter to the specific site at the 5′ terminus of the nascent viral RNA, thus promoting replication and transcription of the viral RNA (21).

We also observed that the polymerase subunits, whether or not they are in a complex with their counterparts, display dramatically reduced mobility compared to that expected for freely diffusing molecules of comparable size. This slow mobility cannot be explained by the formation of higher-order homo-oligomers, since single subunits and the PB1/PA dimer only show a very limited tendency for homo-oligomerization. Furthermore, the ~35% increase in molecular brightness observed by PCH for the PA-mEGFP/PB1-mCFP/mCherry-PB2 complex in the nucleus compared to PA-mEGFP expressed alone suggests that only a minor fraction of the polymerases are forming higher-order oligomers. In contrast, all the poly-

merases should be engaged in homo-oligomers of more than 100 polymerases to account for the very slow diffusion of the PB2/PB1/PA complex. These observations imply that the polymerase subunits or combinations of them always exist within large, slowly diffusing complexes with host factors. It is obviously important to identify these host factors or structures, as they probably play an important role in the transport, assembly, and function of the viral polymerase. Candidates are transport factors such as HSP90 (30), importin α (13), and RanBP5 (8), as well as RNA polymerase II (11, 36), the polyadenylation machinery (24), and chromatin (14).

Conclusions. Taken together, our direct *in vivo* evidence allows us to define a working model for influenza virus polymerase import and assembly. Our data show that the model originally suggested by Deng and coauthors based on indirect evidence (9) indeed applies to living cells. The PB1/PA heterodimer is imported into the nucleus by RanBP5, a member of importin β family (8). In the nucleus, PB1/PA associates with PB2, which is imported independently by importin α (13, 46) to form the fully assembled trimeric polymerase. We demonstrate that NLS-mediated PB2 import is required to accumulate PB1 and PA in the nucleus and prevent aberrant presence of the trimeric polymerase in the cytoplasm. These insights illustrate the power of FCCS to monitor the interactions of viral polymerase subunits *in vivo*. This method promises to be invaluable to study polymerase function and interactions with host factors in the future, as well as to determine the molecular consequences of host range mutations of influenza virus.

ACKNOWLEDGMENTS

We are grateful to S. Terjung, M. Wachsmuth, and C. Maeder for technical assistance with the microscope used for FCCS experiments and to Leica Microsystems for continuous support of the Advanced Light Microscopy Facility at the European Molecular Biology Laboratory (EMBL), Heidelberg. We also thank J. Ortin and N. Naffakh for useful discussions and technical help.

S.H. and S.A. were supported by fellowships from the European Molecular Biology Organization and from the EMBL Interdisciplinary Postdocs Programme (EIPOD), respectively. L.F. was funded by the ANR FLU INTERPOL contract (ANR-06-MIME-014-02).

REFERENCES

1. **Akkina, R. K., T. M. Chambers, D. R. Londo, and D. P. Nayak.** 1987. Intracellular localization of the viral polymerase proteins in cells infected with influenza virus and cells expressing PB1 protein from cloned cDNA. J. Virol. **61:**2217–2224.
2. **Boulo, S., H. Akarsu, R. W. Ruigrok, and F. Baudin.** 2007. Nuclear traffic of influenza virus proteins and ribonucleoprotein complexes. Virus Res. **124:** 12–21.
3. **Chase, G., T. Deng, E. Fodor, B. W. Leung, D. Mayer, M. Schwemmle, and G. Brownlee.** 2008. Hsp90 inhibitors reduce influenza virus replication in cell culture. Virology **377:**431–439.
4. **Chen, Y., J. D. Muller, P. T. So, and E. Gratton.** 1999. The photon counting histogram in fluorescence fluctuation spectroscopy. Biophys. J. **77:**553–567.
5. **Ciruela, F.** 2008. Fluorescence-based methods in the study of protein-protein interactions in living cells. Curr. Opin. Biotechnol. **19:**338–343.
6. **Dawood, F. S., S. Jain, L. Finelli, M. W. Shaw, S. Lindstrom, R. J. Garten, L. V. Gubareva, X. Xu, C. B. Bridges, and T. M. Uyeki.** 2009. Emergence of a novel swine-origin influenza A (H1N1) virus in humans. N. Engl. J. Med. **360:**2605–2615.
7. **de la Luna, S., C. Martinez, and J. Ortin.** 1989. Molecular cloning and sequencing of influenza virus A/Victoria/3/75 polymerase genes: sequence evolution and prediction of possible functional domains. Virus Res. **13:**143–155.
8. **Deng, T., O. G. Engelhardt, B. Thomas, A. V. Akoulitchev, G. G. Brownlee, and E. Fodor.** 2006. Role of ran binding protein 5 in nuclear import and assembly of the influenza virus RNA polymerase complex. J. Virol. **80:** 11911–11919.
9. **Deng, T., J. Sharps, E. Fodor, and G. G. Brownlee.** 2005. In vitro assembly of PB2 with a PB1-PA dimer supports a new model of assembly of influenza A virus polymerase subunits into a functional trimeric complex. J. Virol. **79:**8669–8674.
10. **Eigen, M., and R. Rigler.** 1994. Sorting single molecules: application to diagnostics and evolutionary biotechnology. Proc. Natl. Acad. Sci. U. S. A. **91:**5740–5747.
11. **Engelhardt, O. G., M. Smith, and E. Fodor.** 2005. Association of the influenza A virus RNA-dependent RNA polymerase with cellular RNA polymerase II. J. Virol. **79:**5812–5818.
12. **Fodor, E., and M. Smith.** 2004. The PA subunit is required for efficient nuclear accumulation of the PB1 subunit of the influenza A virus RNA polymerase complex. J. Virol. **78:**9144–9153.
13. **Gabriel, G., A. Herwig, and H. D. Klenk.** 2008. Interaction of polymerase subunit PB2 and NP with importin alpha1 is a determinant of host range of influenza A virus. PLoS Pathog. **4:**e11.
14. **Garcia-Robles, I., H. Akarsu, C. W. Muller, R. W. Ruigrok, and F. Baudin.** 2005. Interaction of influenza virus proteins with nucleosomes. Virology **332:**329–336.
15. **Gonzalez, S., T. Zurcher, and J. Ortin.** 1996. Identification of two separate domains in the influenza virus PB1 protein involved in the interaction with the PB2 and PA subunits: a model for the viral RNA polymerase structure. Nucleic Acids Res. **24:**4456–4463.
16. **Hatta, M., Y. Hatta, J. H. Kim, S. Watanabe, K. Shinya, T. Nguyen, P. S. Lien, Q. M. Le, and Y. Kawaoka.** 2007. Growth of H5N1 influenza A viruses in the upper respiratory tracts of mice. PLoS Pathog. **3:**1374–1379.
17. **Hemerka, J. N., D. Wang, Y. Weng, W. Lu, R. S. Kaushik, J. Jin, A. F. Harmon, and F. Li.** 2009. Detection and characterization of influenza A virus PA-PB2 interaction through a bimolecular fluorescence complementation assay. J. Virol. **83:**3944–3955.
18. **Honda, A., and A. Ishihama.** 1997. The molecular anatomy of influenza virus RNA polymerase. Biol. Chem. **378:**483–488.
19. **Jones, I. M., P. A. Reay, and K. L. Philpott.** 1986. Nuclear location of all three influenza polymerase proteins and a nuclear signal in polymerase PB2. EMBO J. **5:**2371–2376.
20. **Jorba, N., E. Area, and J. Ortin.** 2008. Oligomerization of the influenza virus polymerase complex in vivo. J. Gen. Virol. **89:**520–524.
21. **Jorba, N., R. Coloma, and J. Ortin.** 2009. Genetic trans-complementation establishes a new model for influenza virus RNA transcription and replication. PLoS Pathog. **5:**e1000462.
22. **Kettling, U., A. Koltermann, P. Schwille, and M. Eigen.** 1998. Real-time enzyme kinetics monitored by dual-color fluorescence cross-correlation spectroscopy. Proc. Natl. Acad. Sci. U. S. A. **95:**1416–1420.
23. **Kohl, T., E. Haustein, and P. Schwille.** 2005. Determining protease activity in vivo by fluorescence cross-correlation analysis. Biophys. J. **89:**2770–2782.
24. **Kuo, R. L., and R. M. Krug.** 2009. Influenza A virus polymerase is an integral component of the CPSF30-NS1A protein complex in infected cells. J. Virol. **83:**1611–1616.
25. **Labadie, K., E. Dos Santos Afonso, M. A. Rameix-Welti, S. van der Werf, and N. Naffakh.** 2007. Host-range determinants on the PB2 protein of influenza A viruses control the interaction between the viral polymerase and nucleoprotein in human cells. Virology **362:**271–282.
26. **Li, C., M. Hatta, S. Watanabe, G. Neumann, and Y. Kawaoka.** 2008. Compatibility among polymerase subunit proteins is a restricting factor in the reassortment between equine H7N7 and human H3N2 viruses. J. Virol.
27. **Maeder, C. I., M. A. Hink, A. Kinkhabwala, R. Mayr, P. I. Bastiaens, and M. Knop.** 2007. Spatial regulation of Fus3 MAP kinase activity through a reaction-diffusion mechanism in yeast pheromone signalling. Nat. Cell Biol. **9:**1319–1326.
28. **Magde, D., E. Elson, and W. W. Webb.** 1972. Thermodynamic fluctuations in a reacting system—measurement by fluorescence correlation spectroscopy. Phys. Rev. Lett. **29:**705–708.
29. **Mukaigawa, J., and D. P. Nayak.** 1991. Two signals mediate nuclear localization of influenza virus (A/WSN/33) polymerase basic protein 2. J. Virol. **65:**245–253.
30. **Naito, T., F. Momose, A. Kawaguchi, and K. Nagata.** 2007. Involvement of Hsp90 in assembly and nuclear import of influenza virus RNA polymerase subunits. J. Virol. **81:**1339–1349.
31. **Nath, S. T., and D. P. Nayak.** 1990. Function of two discrete regions is required for nuclear localization of polymerase basic protein 1 of A/WSN/33 influenza virus (H1 N1). Mol. Cell. Biol. **10:**4139–4145.
32. **Nieto, A., S. de la Luna, J. Barcena, A. Portela, and J. Ortin.** 1994. Complex structure of the nuclear translocation signal of influenza virus polymerase PA subunit. J. Gen. Virol. **75:**29–36.
33. **Noah, D. L., and R. M. Krug.** 2005. Influenza virus virulence and its molecular determinants. Adv. Virus Res. **65:**121–145.
34. **Perroud, T. D., B. Huang, and R. N. Zare.** 2005. Effect of bin time on the photon counting histogram for one-photon excitation. Chemphyschem **6:**905–912.
35. **Poole, E., D. Elton, L. Medcalf, and P. Digard.** 2004. Functional domains of the influenza A virus PB2 protein: identification of NP- and PB1-binding sites. Virology **321:**120–133.

36. **Rameix-Welti, M. A., A. Tomoiu, E. Dos Santos Afonso, S. van der Werf, and N. Naffakh.** 2009. Avian influenza A virus polymerase association with nucleoprotein, but not polymerase assembly, is impaired in human cells during the course of infection. J. Virol. **83:**1320–1331.
37. **Resa-Infante, P., N. Jorba, N. Zamarreno, Y. Fernandez, S. Juarez, and J. Ortin.** 2008. The host-dependent interaction of alpha-importins with influenza PB2 polymerase subunit is required for virus RNA replication. PLoS One **3:**e3904.
38. **Rigler, R., Z. Foldes-Papp, F. J. Meyer-Almes, C. Sammet, M. Volcker, and A. Schnetz.** 1998. Fluorescence cross-correlation: a new concept for polymerase chain reaction. J. Biotechnol. **63:**97–109.
39. **Schwille, P., U. Haupts, S. Maiti, and W. W. Webb.** 1999. Molecular dynamics in living cells observed by fluorescence correlation spectroscopy with one- and two-photon excitation. Biophys. J. **77:**2251–2265.
40. **Schwille, P., F. J. Meyer-Almes, and R. Rigler.** 1997. Dual-color fluorescence cross-correlation spectroscopy for multicomponent diffusional analysis in solution. Biophys. J. **72:**1878–1886.
41. **Shaner, N. C., R. E. Campbell, P. A. Steinbach, B. N. Giepmans, A. E. Palmer, and R. Y. Tsien.** 2004. Improved monomeric red, orange and yellow fluorescent proteins derived from Discosoma sp. red fluorescent protein. Nat. Biotechnol. **22:**1567–1572.
42. **Slaughter, B. D., J. W. Schwartz, and R. Li.** 2007. Mapping dynamic protein interactions in MAP kinase signaling using live-cell fluorescence fluctuation spectroscopy and imaging. Proc. Natl. Acad. Sci. U. S. A. **104:**20320–20325.
43. **Smith, G. L., J. Z. Levin, P. Palese, and B. Moss.** 1987. Synthesis and cellular location of the ten influenza polypeptides individually expressed by recombinant vaccinia viruses. Virology **160:**336–345.
44. **Snapp, E. L., R. S. Hegde, M. Francolini, F. Lombardo, S. Colombo, E. Pedrazzini, N. Borgese, and J. Lippincott-Schwartz.** 2003. Formation of stacked ER cisternae by low affinity protein interactions. J. Cell Biol. **163:**257–269.
45. **Sugiyama, K., E. Obayashi, A. Kawaguchi, Y. Suzuki, J. R. Tame, K. Nagata, and S. Y. Park.** 2009. Structural insight into the essential PB1-PB2 subunit contact of the influenza virus RNA polymerase. EMBO J. **28:**1803–1811.
46. **Tarendeau, F., J. Boudet, D. Guilligay, P. J. Mas, C. M. Bougault, S. Boulo, F. Baudin, R. W. Ruigrok, N. Daigle, J. Ellenberg, S. Cusack, J. P. Simorre, and D. J. Hart.** 2007. Structure and nuclear import function of the C-terminal domain of influenza virus polymerase PB2 subunit. Nat. Struct. Mol. Biol. **14:**229–233.
47. **Torreira, E., G. Schoehn, Y. Fernandez, N. Jorba, R. W. Ruigrok, S. Cusack, J. Ortin, and O. Llorca.** 2007. Three-dimensional model for the isolated recombinant influenza virus polymerase heterotrimer. Nucleic Acids Res. **35:**3774–3783.
48. **Toyoda, T., D. M. Adyshev, M. Kobayashi, A. Iwata, and A. Ishihama.** 1996. Molecular assembly of the influenza virus RNA polymerase: determination of the subunit-subunit contact sites. J. Gen. Virol. **77:**2149–2157.
49. **Webster, R. G., W. J. Bean, O. T. Gorman, T. M. Chambers, and Y. Kawaoka.** 1992. Evolution and ecology of influenza A viruses. Microbiol. Rev. **56:**152–179.
50. **World Health Organization.** 2007. Cumulative number of confirmed human cases of avian influenza A/(H5N1) reported to WHO, 2 April 2007. World Health Organization, Geneva, Switzerland.
51. **Young, M. E., P. A. Carroad, and R. L. Bell.** 1980. Estimation of diffusion-coefficients of proteins. Biotechnol. Bioeng. **22:**947–955.
52. **Zimmermann, T.** 2005. Spectral imaging and linear unmixing in light microscopy. Adv. Biochem. Eng. Biotechnol. **95:**245–265.